EURASIAN PHYSICAL TECHNICAL JOURNAL

2026, Volume 23, No. 1 (55)

https://doi.org/10.31489/2026N1/6-14

Received: 16/02/2025 Revised: 14/01/2026 Accepted: 19/03/2026 Published online: 30/03/2026

Research Article

UDC 621.793: 669.14

ELECTRIC ARC SPRAYING WITH COPPER-PLATED WIRE SV08G2S ON GRADE 45 STEEL: FORMATION OF THE STRUCTURE AND PROPERTIES OF PROTECTIVE COATINGS

Sagdoldina Zh.B. [1,2], Leonidova A.B.*[2], Zhassulan A.Zh.[2], Shynarbek A.B.[2], Ibragimov N.K.[2], Mukhametov Y.M.[2]

[1] Sarsen Amanzholov East Kazakhstan University, Ust-Kamenogorsk, Kazakhstan

[2] Shakarim University, Semey, Kazakhstan

*Corresponding author: aiymleonidova1994@gmail.com

Abstract. *The paper investigates the influence of electric arc spraying process parameters using copper-plated Sv08G2S wire on the structure and performance characteristics of coatings formed on grade 45 steel. Spraying was performed at varying voltages and wire feed speeds, followed by a comprehensive analysis of the structure and properties of the resulting coatings. The best coating characteristics were achieved at 40 V, 280 A and a wire feed speed of 100 mm/s: the resulting coating exhibited a relatively dense and uniform structure, high microhardness (277.6 HV), minimal mass loss due to abrasive wear (0.018 g), and enhanced corrosion resistance. Electrochemical tests in a 3.5 wt.% NaCl solution revealed a positive shift of the corrosion potential to −0.318 V (vs. Ag/AgCl) and a low corrosion current density of 4.61 × 10^{-5} A/cm², corresponding to a corrosion rate of 0.54 mm/year. It is shown that voltage is one of the key parameters in supersonic arc metallization, governing arc stability, spray uniformity, and coating quality, whereas increasing the current and wire feed speed resulted in a thicker sprayed layer but promoted pore formation and reduced structural homogeneity. Overall, optimization of spraying parameters enables the formation of high-quality coatings with improved wear and corrosion resistance, thereby increasing the service life of steel components in practical applications.*

Keywords: electric arc spraying, copper-plated wire, grade 45 steel, microhardness, corrosion resistance, wear resistance.

1. Introduction

Grade 45 steel is one of the most widely used carbon structural steels in mechanical engineering, power engineering, and related industries for the manufacture of components due to its combination of strength, affordability, and manufacturability [1]. During operation, under conditions of friction and abrasive action, parts made of grade 45 steel (such as shafts and gears in thermal power plant equipment) undergo accelerated wear, significantly reducing their service life. To enhance the durability and reliability of such components, surface modification methods must be applied to improve their performance characteristics. Among existing technologies, thermal spraying (TS) is of particular interest as it allows the formation of functional coatings without significant thermal deformation of the substrate or changes in the structure of the base material [2, 3]. A key advantage of this technology is the wide selection of usable materials, which ensures versatility in addressing tasks related to improving wear and corrosion resistance. The main types of thermal spraying include flame, detonation, plasma, cold gas-dynamic, electric arc spraying, and other methods [4–12]. Among

these, electric arc spraying (EAS) has attracted particular attention from researchers due to its technological simplicity, low cost, and high productivity. According to technical and economic estimates, coatings obtained by this method are 3–10 times cheaper than similar coatings applied by other thermal spray methods, while maintaining comparable performance characteristics [10–14]. The efficiency of electric arc spraying is largely determined by process parameters, including the material feed rate, current, voltage, air pressure, and spraying distance. These factors directly influence the coating's structure, porosity, microhardness, and adhesion to the substrate [11, 15–18]. In recent years, particular attention has been paid to optimizing spraying conditions, which has significantly improved the wear and corrosion resistance of coatings [18–23].

Along with process parameters, the choice of spray material is a key factor. Among metallic coating materials, copper and its alloys are of particular interest due to their high ductility and excellent thermal and electrical conductivity. When using copper-plated wire, the copper layer facilitates stable arc formation, improves the thermal regime of the process, and ensures more uniform coating deposition. In addition, copper-plated coatings demonstrate high corrosion resistance and can enhance the mechanical properties of the surface. Thus, pseudo-alloys of the Cu–Fe system obtained by arc spraying form dense coatings with low porosity, a microhardness of approximately 2,1 ± 0,7 GPa, and high resistance in aggressive environments, including a 3% NaCl solution [24]. The use of copper-plated wire in arc spraying combines technological simplicity and cost-effectiveness, ensuring the formation of coatings with a range of protective and functional properties.

Thus, the potential of copper-based coatings is confirmed by modern research on composites based on them, which demonstrate improved wear resistance and corrosion protection. The purpose of this study is to identify the formation patterns of copper-plated Sv08G2S wire coatings on the surface of grade 45 steel, with the aim of improving its performance.

2. Materials and Research Methods

In this study, grade 45 steel and copper-plated Sv08G2S wire were used. Their chemical composition (in wt.%) is shown in Table 1 according to GOST 1050–2013. Electric arc spraying was carried out using a Metalcoat system (Figure 1) comprising an Arc Spray Torch (model 100AD) and a power source with control console (model VCH 400 AIR and DC), produced by Metalcoat. The process parameters for arc spraying are given in Table 2. For the experiment, a round disk specimen (66 mm in diameter and 5 mm thick) was prepared and subsequently divided into four equal sectors. Three of these sectors were used for coating deposition and subsequent analyses. Prior to coating, each specimen's surface was ground with 120-grit abrasive paper and then sandblasted, resulting in an initial surface roughness of 0,94 ± 0,12 μm.

Table 1. Chemical composition of materials (wt.%)

Material	C	Si	Mn	S	P	Ni	Cr	Cu
Steel 45	0,42–0,50	0,17–0,37	0,5–0,8	≤0,035	≤0,03	≤0,3	≤0,25	≤0,25
Sv08G2S	0,05–0,11	0,70–0,95	1,8–2,1	≤0,025	≤0,03	≤0,25	≤0,20	≤0,25

After spraying the copper-plated wire onto the grade 45 steel surface, a comprehensive study of the coating's structure and properties was conducted. Coating morphology was examined using a JSM-6390LV scanning electron microscope (JEOL, Tokyo, Japan). To study the coating's structure and porosity, a cross-section of a coated sample was prepared by grinding with abrasive paper up to 2500 grit, followed by polishing on felt wheels using diamond pastes with particle sizes of 0,3 μm and 0,1 μm. Coating porosity was then assessed by analyzing SEM cross-sectional images using ImageJ software (version 1.54d). Surface roughness measurements were performed using an Anytester HY2300 profilometer (Hefei, China). Roughness values (Ra) were determined as the average of 10 measurements taken at different points on the surface. Coating microhardness was measured using an HLV-1DT Vickers microhardness tester with a 1 N indenter load and a dwell time of 10 s. Abrasive wear tests were conducted in accordance with GOST 23.208–79. Electro corundum abrasive (grain size 16-P as per GOST 3647–80) with a relative moisture content of no more than 0.15% was used. The roller rotation frequency was 60 ± 2 min^{-1}, and the sample load was 44,1 ± 0,25 N. According to GOST 23.208–79, since the test material's microhardness did not exceed 400 HV, the number of revolutions was set to 600. Upon completion of the tests, the samples were blown with compressed air, wiped with alcohol, dried, and weighed on an analytical balance with an accuracy of 0.001 g.

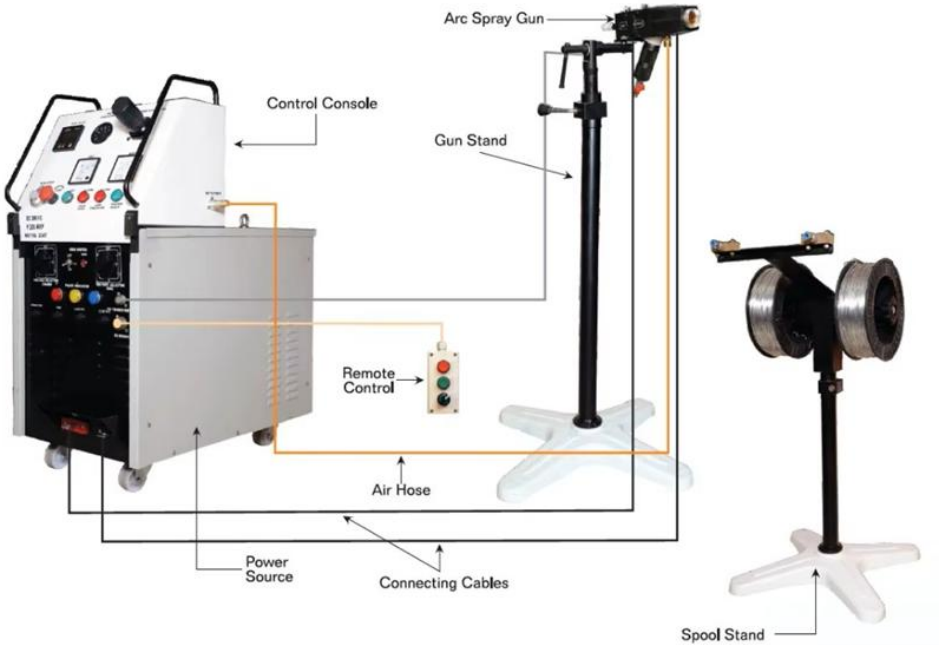

Fig.1. Metalcoat electric arc spraying system.

Table 2. Parameters of the electric arc spraying process.

Sample	U (V)	Wire feed speed (mm/s)	I (A)	Air pressure (MPa)	Distance (mm)	Spraying time (s)
No. 1	30	150	350	0.4	150	5
No. 2	40	100	280	0.4	150	5
No. 3	20	120	300	0.4	150	5

Corrosion resistance was assessed by potentiodynamic polarization using a CS300M potentiostat–galvanostat (Corrtest Instruments, Wuhan, China) with a CS936 flat corrosion cell in a standard three-electrode setup. The working electrode was a coated or uncoated sample with an exposed area of 1 cm². A saturated Ag/AgCl electrode served as the reference and a platinum mesh as the counter-electrode. Tests were carried out in a 3,5 wt% NaCl solution at 25 °C (room temperature). Before polarization, the open-circuit potential was stabilized for 30 min. The corrosion test was performed according to ASTM G5–13.

3. Results and Discussion

Figure 2 shows cross-sectional images of the coatings. As shown in Figure 2 (a–c), the coating thickness varies depending on the process parameters (Table 3). The coating on sample No. 1 has a significant thickness of 778,74 ± 9,26 μm and shows increased layer waviness along the edges. This effect is due to the combination of high current (350 A) and high wire feed speed (150 mm/s), which accelerate the particles and increase the material flow rate, resulting in more material being deposited in a short time. Sample No. 2 exhibited the most uniform structure, with a consistently distributed coating and a thickness of 604,04 ± 15,94 μm. The coating–substrate interface in sample 2 was clearly defined and even. Sample No. 3 had the smallest coating thickness, 326,70 ± 36,03 μm.

The moderate wire feed speed (120 mm/s) combined with the low voltage (20 V) led to incomplete atomization of the material, causing some of the wire to be wasted and preventing proper coating formation on the sample surface. Coating No. 1 is characterized by a low porosity (1.65%) but a relatively large average pore size of 0,863 ± 0,347 μm (Table 3). This is due to the intense deposition of molten particles at high current and high wire feed speed. The resulting jet turbulence and incomplete overlap of individual splat zones contribute to the formation of isolated large pores.

For sample No. 2, the combination of high voltage (40 V) and low wire feed speed produced a large number of small, closed pores. This explains its higher overall porosity (2,575%), with an average pore size of

0,325 ± 0,535 μm. A higher voltage increases the energy transferred to the particles and prolongs their time in a molten state in the spray plume.

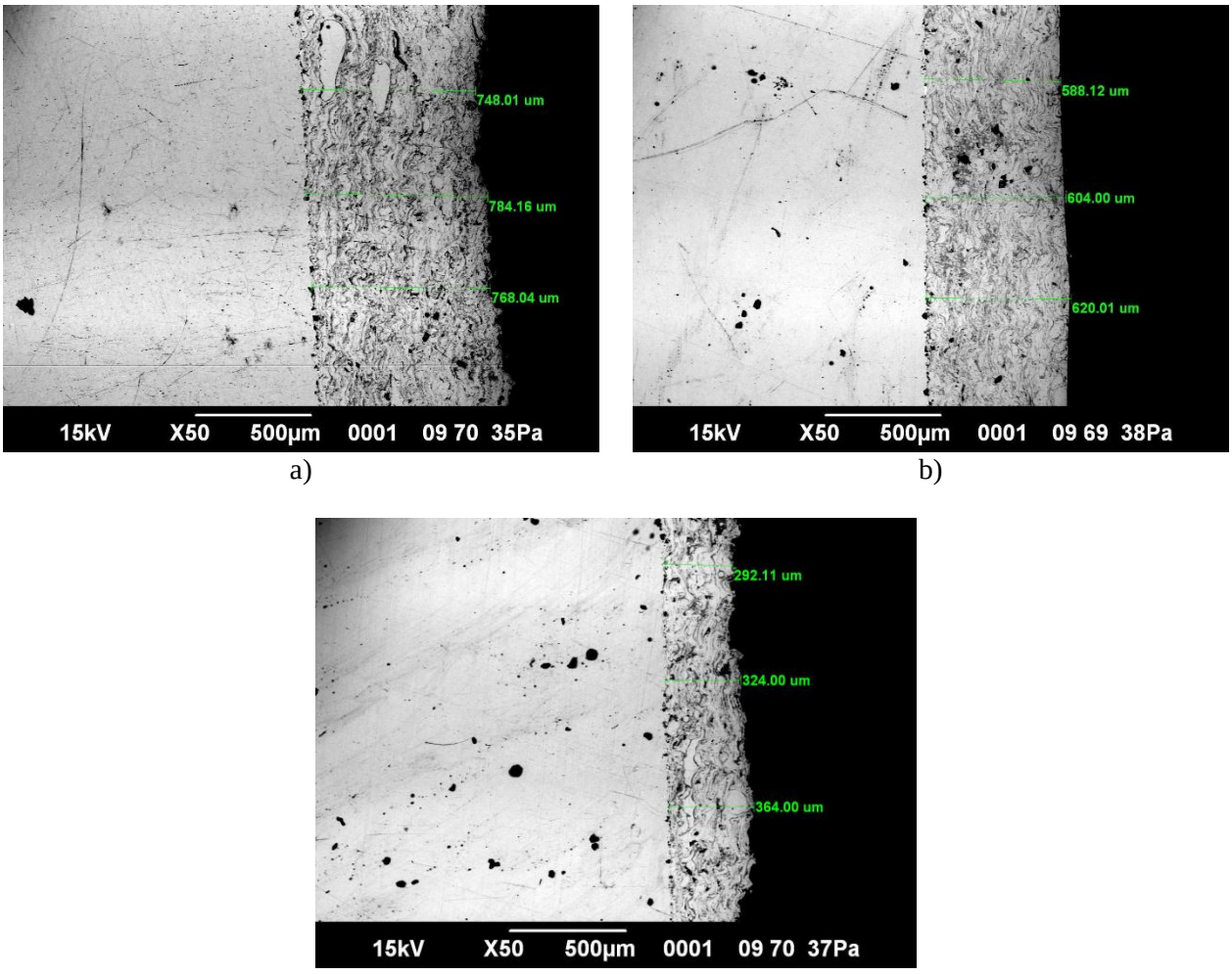

Fig.2. Cross-sectional images of coatings: (a) sample No. 1; (b) sample No. 2; (c) sample No. 3.

Table 3. Coating characteristics.

Sample	Coating thickness (μm)	Average pore size (μm)	Porosity (%)	Roughness Ra (μm)
No. 1	778,74 ± 9,26	0,863 ± 0,347	1,165	11,48 ± 2,01
No. 2	604,04 ± 15,94	0,325 ± 0,535	2,575	7,70 ± 1,41
No. 3	326,70 ± 36,03	0,146 ± 0,264	0,953	5,28 ± 0,68

This raises the likelihood of chemical interaction with oxygen, leading to the formation of oxides and gaseous products. These oxides and gases become incorporated into the molten phase or are released during solidification, remaining as closed or semi-open pores within the coating. Sample No. 3 is characterized by the lowest porosity (0,953%) and the smallest average pore size, 0,146 ± 0,264 μm. Reducing the particle dispersion energy lowers the likelihood of air entrapment and defect formation, resulting in only very small pores. The low voltage (20 V) decreases the degree of particle melting and the residence time of particles in the arc, which minimizes oxidation and gas inclusion formation; as a result, the overall porosity of the coating is minimal. Similar correlations between spraying parameters and coating porosity have been reported in the literature [24-26].

Table 3 also presents the surface roughness (Ra) values for the samples. After coating application, the roughness increased significantly: for sample No. 1, Ra = 11,48 ± 2,01 μm; for sample No. 2, Ra = 7,70 ± 1,41 μm; and for sample No. 3, Ra = 5,28 ± 0,68 μm. Sample No. 1 had the highest roughness, while sample No. 3 had the lowest, indicating that the process parameters significantly influence the formation of the surface

microrelief. Voltage plays a key role in supersonic arc spraying, as it affects arc stability and intensity. At an optimal voltage, the arc remains stable, facilitating uniform metal spraying and the formation of a high-quality coating. If the voltage is too low, the arc can become unstable and intermittent, leading to an uneven coating [12–15]. Surface roughness and coating porosity are also key factors in wear mechanisms and can influence the development of abrasive wear. The abrasive wear test results are presented in Table 4. Sample No. 3 showed the greatest mass loss, indicating the lowest wear resistance of the coating produced under those spraying conditions. This is possibly due to the highly porous structure of that coating. During abrasive wear, the pores can facilitate accelerated material removal, leading to greater mass loss. In contrast, the minimal mass loss observed for sample No. 2 (0,018 g) demonstrates the effectiveness of the chosen spraying parameters in ensuring high wear resistance of the coating.

Table 4. Results of coating abrasive wear testing.

Sample	Mass before (g)	Mass after (g)	Mass loss (g)
No. 1	28,555	28,530	0,025
No. 2	31,556	31,538	0,18
No. 3	24,972	24,936	0,036

The microhardness measurements of the samples are shown in Figure 3. These average values (with corresponding errors) indicate a substantial increase in surface microhardness compared to the original grade 45 steel. The coating microhardness exceeds that of the uncoated material (grade 45 steel, ~190 HV). In particular, sample No. 1 had a microhardness of 242,87 ± 10,89 HV; sample No. 2, 277.62 ± 4,67 HV; and sample No. 3, 272.81 ± 10,52 HV. These data demonstrate an improvement in the surface's strength characteristics after applying the coatings.

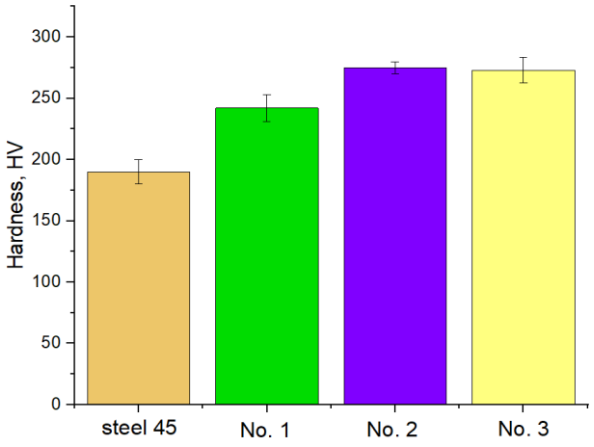

Fig. 3. Microhardness values of the samples.

The increased microhardness of the coatings (relative to the original steel) can be attributed to specific features of the electric arc metallization process. Specifically, when molten metal particles impact the substrate surface, they are rapidly cooled by the cold compressed air jet, causing nearly instantaneous solidification and the formation of a structure with higher microhardness [27]. In sample No. 1, the high current (350 A) led to significant heat input in the spray zone, potentially causing particle overheating, burnout of alloying elements, and intense oxidation of the molten surface. The increased wire feed speed (150 mm/s) reduced the specific energy per unit mass of metal, limiting the extent of uniform melting. The combination of these factors resulted in a coating with partially unmelted and overheated particles, yielding a relatively low microhardness of 242,87 ± 10,89 HV for sample No. 1.

Sample No. 2 exhibited an optimal balance of voltage (40 V) and current (280 A) at a moderate wire feed speed (100 mm/s). As a result, the specific heating energy was sufficient for complete particle melting, leading to the formation of a dense coating structure with the maximum microhardness (277,62 ± 4,67 HV) among the samples. Sample No. 3 was characterized by minimal heat input, which affected the morphology of the

resulting coating. In its structure, dense inclusions visually resembling unmelted material were observed (Figure 2c). These inclusions were uniformly distributed across the cross-section and reduced the overall porosity. As a result of these structural features, sample No. 3 still demonstrated a high microhardness of 272,81 ± 10,52 HV. It can be seen that the balance between the applied arc energy, wire feed speed, and cooling conditions largely determines the coating microhardness. Additionally, factors such as the degree of particle melting, the likelihood of particle overheating and oxidation, and the coating's porosity significantly influence the final microhardness.

Figure 4 shows the polarization curves of grade 45 steel samples in a 3.5% NaCl solution. The uncoated steel sample exhibited a more negative corrosion potential and a higher corrosion current density, indicating low resistance to the chloride environment. After applying the copper-plated wire arc spray coating, a positive shift in corrosion potential and a decrease in current density were observed. This indicates a reduction in the steel's thermodynamic susceptibility to corrosion and a slowing of the electrochemical processes.

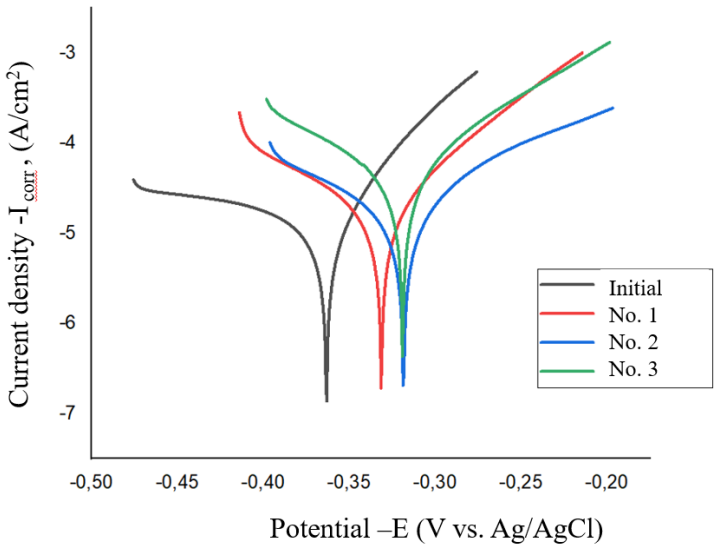

Fig. 4. Potentiodynamic polarization curves of grade 45 steel samples in 3.5% NaCl solution

The most positive shift in corrosion potential and the lowest corrosion current density was observed for sample No. 2, which was obtained with the following parameters: arc air pressure 0,4 MPa, air pressure 0,2 MPa, 40 V, and 280 A. This implies the formation of a denser, less porous coating structure, providing the best corrosion protection. Therefore, the spraying parameters used for sample No. 2 can be considered optimal for producing coatings with enhanced corrosion resistance. The obtained results are consistent with previous studies of arc spray coatings on carbon steels. In particular, the coating thickness (604 ± 15.9 μm) and microhardness (277.6 ± 4.7 HV) observed under optimal spraying conditions (40 V, 280 A, wire feed 100 mm/s) are comparable to the values reported by other authors [28-30]. Moreover, similar to previous studies, the use of wire with this coating resulted in a coating with low porosity, improved wear resistance, and high corrosion resistance in a 3.5% NaCl solution. These comparisons confirm that the selected process parameters are effective in improving the performance and durability of components made of grade 45 steel.

4. Conclusions

This research broadens the potential practical applications of electric arc spraying with copper-plated Sv08G2S wire on grade 45 steel under various spraying conditions.

Process parameters significantly affect the formation of the coating's structure and properties, including its thickness, porosity, surface roughness, microhardness, wear resistance, and corrosion behavior.

Optimal coating characteristics were obtained at 40 V, 280 A and a wire feed rate of 100 mm/s (sample No. 2). Under these conditions, the average coating thickness was 604 ± 15,9 μm, the maximum microhardness was 277,6 ± 4,7 HV, the mass loss due to abrasive wear was minimal (0,018 g), and the coating exhibited high corrosion resistance in a 3,5% NaCl solution.

The coating thickness across the tested modes varied from 327 μm to 779 μm, depending on the spraying parameters. Increasing the current and wire feed speed increased the coating thickness, but also led to larger pores and reduced structural homogeneity. Overall, the results confirm that electric arc spraying with copper-plated wire is an accessible and effective method for improving the performance characteristics and durability of grade 45 steel components in mechanical engineering and related applications.

Conflict of interest statement. The authors declare that the re-search was conducted in the absence of any commercial or financial relationships that could be construed as a potential conflict of interest.

CRediT author statement.
Leonidova A.B.: conceptualization, methodology; **Shynarbek A.B.**: investigation; **Zhassulan A.Zh.**: data curation, visualization; **Ibragimov N.K.**: resources; validation; **Mukhametov Y.M.**: formal analysis; **Leonidova A.B.**: writing-original draft; **Sagdoldina Zh.B.**: writing-review and editing, supervision, project administration. All authors have read and approved the final version of the manuscript.

Funding

This research has been funded by the Committee of Science of the Ministry of Science and Higher Education of the Republic of Kazakhstan (Grant No. BR24992870).

References

1 Li Y., Liu S., Wang Y., Wei Y., Han L., Zhi H., & Yang X. (2023) Effects of process parameters on the microstructure and mechanical properties of AISI 1045 steel prepared by selective laser melting. *Materials Today Communications*, 37, 107287. https://doi.org/10.1016/j.mtcomm.2023.107287

2 Su X., Zhu X., Fu Y., Xiao S., & Liu Y. (2024) Comparative Analysis of Tribological Behavior of 45 Steel under Intensive Quenching-High-Temperature Tempering and Queenching-Tempering Process. *Applied Sciences*, 14(13), 5942. https://doi.org/10.3390/app14135942

3 Davis J. R. (2004) Handbook of thermal spray technology. *ASM international*. Available at: https://books.google.kz/books?id=S0PryYc9T70C&lpg=PA128&ots=m93YUXnCp&dq=Davis%2C%20J.%20R.%20

4 Oksa M., Turunen E., Suhonen T., Varis T., & Hannula S. P. (2011) Optimization and characterization of high velocity oxy-fuel sprayed coatings: techniques, materials, and applications. *Coatings*, 1(1), 17-52. https://doi.org/10.3390/coatings1010017

5 Sunitha K., & Vasudev H. (2022) A short note on the various thermal spray coating processes and effect of post-treatment on Ni-based coatings. *Materials Today: Proceedings*, 50, 1452-1457. https://doi.org/10.1016/j.matpr.2021.09.017

6 Łatka L., Pawłowski L., Winnicki M., Sokołowski P., Małachowska A., & Kozerski S. (2020) Review of functionally graded thermal sprayed coatings. *Applied Sciences*, 10(15), 5153. https://doi.org/10.3390/app10155153

7 Rakhadilov B., Buitkenov D., Sagdoldina Z., Idrisheva Z., Zhamanbayeva M., & Kakimzhanov D. (2021) Preparation and characterization of NiCr/NiCr-Al2O3/Al2O3 multilayer gradient coatings by gas detonation spraying. *Coatings*, 11(12), 1524. https://doi.org/10.3390/coatings11121524

8 Kengesbekov A., Rakhadilov B., Sagdoldina Z., Buitkenov D., Dosymov Y., & Kylyshkanov M. (2022) Improving the efficiency of air plasma spraying of titanium nitride powder. *Coatings*, 12(11), 1644. https://doi.org/10.3390/coatings12111644

9 Fukumoto M. (2008) The current status of thermal spraying in Asia. *Journal of Thermal Spray Technology*, 17(1), 5-13. https://doi.org/10.1007/s11666-008-9154-8

10 Tejero-Martin D., Rezvani Rad M., McDonald A., & Hussain T. (2019) Beyond traditional coatings: a review on thermal-sprayed functional and smart coatings. *Journal of Thermal Spray Technology*, 28(4), 598-644. https://doi.org/10.1007/s11666-019-00857-1

11 Rakhadilov B., Magazov N., Kakimzhanov D., Apsezhanova A., Molbossynov Y., & Kengesbekov A. (2024) Influence of spraying process parameters on the characteristics of steel coatings produced by arc spraying method. *Coatings*, 14(9), 1145. https://doi.org/10.3390/coatings14091145

12 Malek M.H.A., Saad N. H., Abas S. K., & Shah N. B. M. (2014). Critical process and performance parameters of thermal arc spray coating. *International Journal of Materials Engineering Innovation*, 5(1), 12-27. https://doi.org/10.1504/IJMATEI.2014.059489

13 Hauer M., Ripsch B., Gericke A., Krömmer W., & Henkel K.-M. (2023) Advanced Analyses of Heating Elements Manufactured by an Optimized Arc Spraying Process. *Coatings*, 13(10), 1701. https://doi.org/10.3390/coatings13101701

14 Devaraj S., McDonald A., & Chandra S. (2021). Metallization of porous polyethylene using a wire-arc spray process for heat transfer applications. *Journal of Thermal Spray Technology*, 30(1), 145-156. https://doi.org/10.1007/s11666-020-01119-1

15 Tillmann W., Abdulgader M., Wirtz A., Milz M.P., Biermann D., & Walther F. (2022) The Effect of Argon as Atomization Gas on the Microstructure, Machine Hammer Peening Post-Treatment, and Corrosion Behavior of Twin Wire Arc Sprayed (TWAS) ZnAl4 Coatings. *Coatings*, 12(1), 32. https://doi.org/10.3390/coatings12010032

16 Ndumia J. N., Kang M., Gbenontin B. V., Lin J., Liu J., Li H., & Nyambura S. M. (2023) Optimizing parameters of arc-sprayed Fe-based coatings using the response surface methodology. *Journal of Thermal Spray Technology*, 32(7), 2202-2220. https://doi.org/10.1007/s11666-023-01621-2

17 Pham T.H., Nguyen V.T., Le T.Q., Nguyen T.A., Pham T.L., Nguyen T.P., Dao B.T., Ly Q.C., & Le D.T. (2021) Influence of electric arc spraying parameters on the porosity and adhesion strength of Al-Mg alloy coating. *Proceeding of the Intern. Conf. on Advanced Mechanical Engineering, Automation and Sustainable Development*, 655 – 659. Springer International Publishing. https://doi.org/10.1007/978-3-030-99666-6_94

18 Rakhadilov B., Buitkenov D., Apsezhanova A., Kakimzhanov D., Nabioldina A., & Magazov N. (2025) Selection of Optimal Process Parameters for Arc Metallization. *Coatings*, 15(3), 300. https://doi.org/10.3390/coatings15030300

19 Ndumia J.N., Kang M., Gbenontin B.V., Lin J., & Nyambura S. M. (2021). A Review on the Wear, Corrosion and High-Temperature Resistant Properties of Wire Arc-Sprayed Fe-Based Coatings. *Nanomaterials*, 11(10), 2527. https://doi.org/10.3390/nano11102527

20 Wang S., Guo T., Xu G., & Ding F. (2023) Corrosion behavior and mechanism of electric arc-sprayed Al-Mg coating and Zn-Al-Mg pseudo-alloy coatings. *Surface and Coatings Technology*, 475, 130126. https://doi.org/10.1016/j.surfcoat.2023.130126

21 Cooke K., Oliver G., Buchanan V., & Palmer N. (2007) Optimisation of the electric wire arc-spraying process for improved wear resistance of sugar mill roller shells. *Surface and Coatings Technology*, 202(1), 185-188. https://doi.org/10.1016/j.surfcoat.2007.05.015

22 Bang J., & Lee E. (2023) Evaluation of the Mechanical and Corrosion Behavior of Twin Wire Arc Sprayed Ni-Al Coatings with Different Al and Mo Content. *Coatings*, 13(6), 1069. https://doi.org/10.3390/coatings13061069

23 Yury K., Filippov M., Makarov A., Malygina I., Soboleva N., Fantozzi D., Andrea M., Koivuluoto H., & Vuoristo P. (2018). Arc-Sprayed Fe-Based Coatings from Cored Wires for Wear and Corrosion Protection in Power Engineering. *Coatings*, 8(2), 71. https://doi.org/10.3390/coatings8020071

24 Borisov Y. S., Vigilianska N. V., Iantsevitch C. V., & Demianov I. A. (2023) Corrosion resistance of pseudoalloy copper-iron coatings obtained by electric arc spraying. *Materials Science*, 59(2), 223-227. https://doi.org/10.1007/s11003-024-00766-x

25 Boronenkov V., & Korobov Y. (2016). Fundamentals of arc spraying. *Physical and Chemical Regularities*; Springer: Berlin/Heidelberg, Germany. https://doi.org/10.1007/978-3-319-22306-3

26 Tamaki R., & Yamakawa M. (2018) Elucidation of mechanism for reducing porosity in electric arc spraying through CFD. *Proceeding of the Intern. Conf.on Computational Science*, 418 - 428. Springer International Publishing. https://doi.org/10.1007/978-3-319-93698-7_32

27 Rakhadilov B., Shynarbek A., Kusainov R., Kakimzhanov D., Ormanbekov K., & Zhassulan A. (2024) Study of compressed air pressure on the properties of coatings obtained by supersonic metallization. *Journal of Theoretical and Applied Physics*, 18(6). https://doi.org/10.57647/j.jtap.2024.1806.77

28 Isakov S. A., & Lezhava A.G. (2016) Determination of optimal parameters for obtaining metal coatings by electric arc metallization using a current source with a falling volt-ampere characteristic. In New Functional Materials, Modern Technologies and Research Methods (pp. 17-18). https://www.elibrary.ru/download/elibrary_29831895_26071298.pdf [in Russian].

29 Kolyada V. S., & Shakhov V. A. (2017) New technologies and equipment for the restoration of concaves of Claas Tucano combines. Izvestiya Orenburgskogo gosudarstvennogo agrariannogo universiteta, (1 (63)), 80-82. https://cyberleninka.ru/article/n/novye-tehnologii-i-oborudovanie-dlya-vosstanovleniya-podbarabaniy-kombaynov-claas-tucano/viewer [in Russian].

30 Koroteyev A. O., Kulikov V. P., & Dolyachko V. P. (2017) Characteristics of the selection of welding wire for arc welding in Ar+ CO_2 with two-jet coaxal supply of shielding gases to the arc zone. Bulletin of the Belarusian-Russian University, (3 (56)), 65-73. https://cyberleninka.ru/article/n/osobennosti-vybora-svarochnyh-provolok-pri-dugovoy-svarke-v-srede-ar-co2-s-dvuhstruynoy-koaksalnoy-podachey-zaschitnyh-gazov-v-zonu/viewer [in Russian].

AUTHORS' INFORMATION

Sagdoldina, Zhuldyz – PhD, Associate Professor, Sarsen Amanzholov East Kazakhstan State University, Ust-Kamenogorsk, Kazakhstan; Senior Lecturer, Department of Technical Physics and Thermal Power Engineering, Shakarim University, Semey, Kazakhstan; Scopus ID: 24476592900; https://orcid.org/000-0001-6421-2000; sagdoldina@mail.ru

Leonidova, Aiym – PhD student, Research School of Physical and Chemical Sciences, Department of Technical Physics and Heat Power Engineering, Shakarim University, Semey, Kazakhstan; Scopus ID: 60013968800; https://orcid.org/0009-0008-2981-2041; aiymleonidova1994@gmail.com

Zhassulan, Ainur – PhD student, Engineering Center, Research School of Physical and Chemical Sciences, Department of Technical Physics and Heat Power Engineering, Shakarim University, Semey, Kazakhstan; Scopus ID: 58837450200; https://orcid.org/0009-0001-5887-0135; a.zhassulan@shakarim.kz

Shynarbek, Aibek – PhD student, Engineering Center, Shakarim University, Semey, Kazakhstan; Scopus ID: 58838202500; https://orcid.org/0009-0009-2877-5178; Shinarbekov16@gmail.com

Ibragimov, Nadir - Candidate of Technical Sciences, Senior Lecturer, Research School of Engineering, Department of Bioengineering Systems, Shakarim University, Semey, Kazakhstan; Scopus ID: 57188718716; https://orcid.org/0000-0001-9607-823X; n.ibragimov@shakarim.kz

Mukhametov, Yeldos - PhD, Head of the Department, Graduate school of STEAM education, Department of Physics and Informatics, Shakarim University, Semey, Kazakhstan; Scopus ID:59654975600; https://orcid.org/0000-0001-7818-8160; y.mukhametov@shakarim.kz